Atomistic spin dynamics of the Cu-Mn spin-glass alloy

B. Skubic,[1] O. E. Peil,[1,2,*] J. Hellsvik,[1] P. Nordblad,[3] L. Nordström,[1] and O. Eriksson[1]
[1]*Department of Physics and Materials Science, Uppsala University, P.O. Box 530, SE-751 21 Uppsala, Sweden*
[2]*Department of Materials Science and Engineering, KTH, SE-100 44 Stockholm, Sweden*
[3]*Department of Engineering Sciences, Uppsala University, P.O. Box 534, SE-751-21 Uppsala, Sweden*
(Received 11 September 2008; published 9 January 2009)

We demonstrate the use of Langevin spin dynamics for studying dynamical properties of an archetypical spin-glass system. Simulations are performed on CuMn (20% Mn) where we study the relaxation that follows a sudden quench of the system to the low-temperature phase. The system is modeled by a Heisenberg Hamiltonian where the Heisenberg interaction parameters are calculated by means of first-principles density-functional theory. Simulations are performed by numerically solving the Langevin equations of motion for the atomic spins. It is shown that dynamics is governed, to a large degree, by the damping parameter in the equations of motion and the system size. For large damping and large system sizes, we observe the typical aging regime.

DOI: 10.1103/PhysRevB.79.024411 PACS number(s): 75.50.Lk, 75.40.Mg, 75.10.Nr

I. INTRODUCTION

Spin glasses exhibit exotic dynamical properties such as aging, memory, and rejuvenation, which have triggered a lot of research in the past.[1,2] The interest in dynamics in these systems is mainly motivated by the fact that practically only out-of-equilibrium properties of spin glasses can be observed in experiments. Peculiarities in the dynamical behavior are often related to a complex nature of the phase space and the lack of ergodicity in spin-glass systems.[3] In particular, relaxation toward equilibrium is not characterized by a single time scale but rather by a broad spectrum of relaxation times leading to a nontrivial evolution of measurable quantities, such as, e.g., magnetization.

An aging experiment is an elegant way to reveal the multiscale nature of the spin-glass dynamics.[4] A system is prepared by quenching from high temperatures to a given temperature T and perturbing the system in some way, usually by switching on an external magnetic field. A measurement of the time evolution of the magnetization is performed after a certain time, t_w, has passed since the system preparation. For temperatures T below the spin-glass transition temperature T_g, relaxation of the magnetization toward the equilibrium value shows a strong dependence on the waiting time, t_w. A number of phenomenological models have been proposed to explain this behavior, among which are the well-known droplet model[5] and a class of hierarchical models.[6–10] However, scaling laws resulting from these studies do not allow interpretation of experimental results unambiguously since this would require an access to asymptotic regimes of relaxation and hence enormously large time scales. Moreover, different, sometimes even contradicting, models give rise to the same scaling laws, discrediting their predictions. Studying generic models seems therefore to be a more promising way to elucidate mechanisms underlying spin-glass dynamics.

The microscopic structure of disordered magnetic materials can, in general, be rather complicated (such as in amorphous spin glasses) but many important features of a spin-glass behavior are captured in a model proposed by Edwards and Anderson[11] and its various extensions (hereafter referred to as "EA models"). This class of models has been studied extensively and, in particular, much attention has been paid to their nonequilibrium behavior.[12–20] These numerical studies have shown that the dynamical behavior of the correlation function is very similar to that of the magnetization (related to the correlation function via the fluctuation-dissipation theorem in equilibrium) in experiments. In particular, the two-stage relaxation depending on the waiting time is reproduced in the simulations. Also, effects of spatial inhomogeneity have been shown to play role in spin-glass dynamics.[21–24]

Originally, the EA model and its extensions were intended to reflect the basic ingredients of spin-glass systems, namely, frustration and disorder. It is, however, appealing to study models that rely on the structure of real spin-glass materials because this kind of models may present a good framework in investigating materials specific properties of spin-glass alloys. First steps in this direction were made in early works of Walstedt and Walker[25,26] or more recent works of Matsubara and Iguchi,[27] in which equilibrium properties of a site-diluted model with Ruderman-Kittel-Kasuya-Yosida (RKKY) interactions were studied.

Here we attempt to provide a parameter free model whose dynamics is self-consistently described by atomistic spin dynamics equations with only one external parameter characterizing magnetic damping. We study the spin-glass dynamics of the $Cu_{80}Mn_{20}$ alloy by modeling it with a random-site Heisenberg Hamiltonian,

$$\mathcal{H} = -\sum_{i,j} J_{ij} c_i c_j \mathbf{m}_i \cdot \mathbf{m}_j, \tag{1}$$

where $\mathbf{m}_i$ represent vector magnetic moments, and c_i are the occupation numbers of the magnetic atoms (c_i is equal to one if a site is occupied by a Mn atom and zero otherwise). The exchange parameters, J_{ij}, are calculated accurately within the density-functional theory (DFT) approach, which means that all interatomic exchange parameters and magnetic moments are calculated in a materials specific fashion. Hamiltonian (1) is suitable only for an ideal alloy without impurities, in which anisotropy is negligible. On the other hand, real CuMn

alloys exhibit macroscopic magnetic anisotropy in experiments,[28] which is probably due to the presence of heavy nonmagnetic impurities.[29] In the current work, we, however, neglect the effect of anisotropy on dynamics to simplify analysis of results. At the same time, we assume that a mechanism providing magnetic damping is present in the system. A usual tool for studying dynamics of spin glasses is Monte Carlo simulations.[14–16,18,19,30] Such an approach misses some details of local relaxations of spins in their local fields. The influence of the finite rate of these local relaxations on dynamics can, in general, be investigated by solving the Langevin dynamics equations directly. As a matter of fact, as will be shown below, motion of individual spins can have a rather strong impact on the aging behavior of the system.

In Sec. II, we introduce definitions used throughout the paper and describe briefly the way aging is observed in experiments. In Sec. III, governing equations for the atomistic spin dynamics are given along with some details on the implementation. Results of the numerical simulations of the CuMn alloy and Heisenberg EA model are presented in Sec. IV. The focus is on the influence of damping on the spin dynamics.

II. DEFINITIONS AND THEORY

In a typical aging experiment, a system is quenched in zero field from high temperatures to a temperature below T_g. Then, the system is aged during a waiting time t_w, a small constant field h is applied, and time dependence of the magnetization $M(t)$ or susceptibility $\chi(t)=M(t)/h$ is observed. A relaxation process after the quench can be associated with three phases: (1) an initial relaxation toward a local quasiequilibrium state, (2) aging dynamics, and (3) global equilibration. The latter is achievable only for systems of finite size N (the number of magnetic sites) within a time greater than the ergodic time $\tau_{\mathrm{erg}} \sim \exp(N)$. Although equilibration is of little interest in an experiment, it must be taken into account in numerical simulations when one deals with relatively small systems.

In numerical simulations, it is convenient to work with the autocorrelation function,

$$C(t_w+t,t_w)=\frac{1}{N}\sum_i [\mathbf{m}_i(t_w)\cdot\mathbf{m}_i(t_w+t)]_{\mathrm{av}}, \tag{2}$$

where $[\cdots]_{\mathrm{av}}$ stands for configurational averaging, i.e., averaging over independent runs with randomly generated atomic distributions $\{c_i\}$. In the quasiequilibrium phase, when the conditions for the fluctuation-dissipation theorem (FDT) are fulfilled, the autocorrelation is related to the response function,[2]

$$R(t_w+t,t_w)=-\frac{1}{T}\frac{\partial C(t_w+t,t_w)}{\partial t_w}. \tag{3}$$

Within linear response, the (thermoremanent) magnetization and susceptibility can be found in the following way:

$$M(t_w+t,t_w)=h\int_0^{t_w} dt' R(t_w+t,t'), \tag{4}$$

$$\chi(\omega,t_w)=\int_0^{t_w} dt' R(t_w,t') e^{i\omega(t'-t_w)}, \tag{5}$$

where h is a small applied magnetic field in a corresponding thermoremanent magnetization experiment. In quasiequilibrium, the relaxation of observables does not depend on t_w, and a relation between the magnetization and the autocorrelation function amounts to

$$M(t)=M_0-\frac{h}{T}C_{\mathrm{eq}}(t), \tag{6}$$

where $C_{\mathrm{eq}}(t)\equiv C(t_w+t,t_w)$ in a t_w-independent regime. In a nonequilibrium situation, when the FDT is violated, different stages of the autocorrelation relaxation can be illustrated by the relaxation rate function defined as

$$S(t_w+t,t_w)=-\frac{d}{d\ln t}C(t_w+t,t_w). \tag{7}$$

The relaxation rate peaks at a time t_a of the order of the age of the system, i.e., $t_a \sim t_w$.

Spin dynamics of a spin glass is essentially nonequilibrium, and the aging behavior in particular implies that the evolution of the autocorrelation function is strongly dependent on the waiting time, i.e., time-translation invariance is violated. However, under certain circumstances or during certain time intervals, a condition of time-translation invariance, $C(t_w+t,t_w)=C(t)$, holds, and the relaxation of the system is said to proceed in the quasiequilibrium regime. This assertion can be considered as a definition of a quasiequilibrium state.

After being prepared at a temperature T, the system tends to an equilibrium state. This state can be characterized by a space correlation function that for spin glasses is calculated in the following way:

$$G(R)=\frac{1}{N}\sum_i [(\langle\mathbf{m}_i\cdot\mathbf{m}_{i+R}\rangle-\langle\mathbf{m}_i\rangle\cdot\langle\mathbf{m}_{i+R}\rangle)^2]_{\mathrm{av}}. \tag{8}$$

Above the transition temperature for sufficiently large R, the spatial correlation is given by

$$G(R)\sim R^{d-2+\eta}u(R/\xi), \tag{9}$$

where d is the dimension of the system, η and ξ are a critical exponent and the correlation length, respectively, and $u(x)$ is a scaling function which decays to zero for $R/\xi\to\infty$. In the macroscopic limit, the correlation length ξ is finite above T_g but diverges with $\xi\sim\epsilon^{-\nu}$ as T_g is approached from above, where $\epsilon=(T-T_g)/T_g$ is the reduced temperature and ν is a critical exponent.

III. DESCRIPTION OF METHOD

Generally, equations of motion for the Mn spins in a dilute CuMn alloy involve coupling of the spins with an effective field produced by the conduction-electron bath. Since the effective field is in turn induced by other spins, this coupling becomes a long-range exchange interaction between spins.[31] However, if spin-orbit coupling is taken into ac-

count, additional damping of the spin motion is introduced, which can be described by a phenomenological Landau-Lifshitz-Gilbert (LLG) term in the equations of motion.[32]

Our simulations are performed using the atomic spin dynamics (ASD) package[33] based on an atomistic approach for spin dynamics. We use a parametrization of the interatomic exchange part of the Hamiltonian in the form of Eq. (1). The effect of temperature is modeled by Langevin dynamics. The LLG damping is characterized by a damping parameter α, which is the only parameter in our simulations not obtained from DFT calculations.

The microscopic equations of motion for the atomic moments, $\mathbf{m}_i$, in an effective field, $\mathbf{B}_i$, are expressed as follows:

$$\frac{d\mathbf{m}_i}{dt} = -\gamma \mathbf{m}_i \times [\mathbf{B}_i + \mathbf{b}_i(t)] - \gamma \frac{\alpha}{m} \mathbf{m}_i \times (\mathbf{m}_i \times [\mathbf{B}_i + \mathbf{b}_i(t)]). \tag{10}$$

In this expression γ is the electron gyromagnetic ratio and $\mathbf{b}_i(t)$ is a stochastic magnetic field with a Gaussian distribution. The magnitude of that field is related to the damping parameter, α, allowing the system to eventually reach thermal equilibrium.

The effective field, $\mathbf{B}_i$, on a site i is calculated from

$$\mathbf{B}_i = -\frac{\partial \mathcal{H}}{\partial \mathbf{m}_i}, \tag{11}$$

where for $\mathcal{H}$ we use the classical Heisenberg Hamiltonian defined by Eq. (1). We use the Heuns method (for details, see Ref. 33) with a time step size of 0.01 fs for solving the stochastic differential equations. Most of the calculations are performed up to a time $t=70$ ps.

IV. LANGEVIN SPIN DYNAMICS OF A HEISENBERG SPIN GLASS

A. Spin dynamics of CuMn

Spin dynamic simulations are performed for the CuMn alloy with 20% of magnetic atoms (Mn). The system is described by the Heisenberg Hamiltonian with spins (magnetic atoms) distributed over the fcc lattice. The magnetic exchange (for the Heisenberg Hamiltonian) parameters are obtained by means of the screened generalized perturbation method (Ref. 34) implemented within the exact muffin-tin orbital (Ref. 35) scheme. The coherent-potential approximation and disordered local moments are used to treat the disordered CuMn alloy in the paramagnetic state properly. Preliminary Monte Carlo simulations showed that with this model and for 20% Mn, critical slowing down occurs close to the experimental freezing temperature, T_g, measured to equal approximately 90 K.[36] However, no reliable estimation of the transition temperature has been done in this work but we assume that the temperature of 10 K, at which most calculations are performed, is deep below the transition temperature, which is confirmed by dynamical simulations. In contrast to the EA model, where assumptions are made that bonds between atomic spins are random and the magnetic sites are ordered, we have used interatomic exchange parameters between the Mn atoms calculated from first-principles theory while occupations of atomic sites have been randomly generated. The dependence of the exchange parameters on distance is calculated and observed to follow an oscillatory RKKY-like form. Unlike the original RKKY theory, the angular dependence of the interactions is furthermore involved naturally in the calculations, reflecting crystallographic properties of the underlying lattice. The exchange interactions are assumed to be independent of the local environment, which is motivated by first-principles calculations that show an insignificant variation in the interactions in the random alloy compared to the ordered one. At the same time, the interactions obtained from the calculations accurately reproduce the magnetic short-range order observed in experiments.[37] Simulations are performed on systems containing $32\times32\times32$ elementary cubic cells. We simulate the relaxation process following a quench from completely random spin orientations to 10 K. Averaging is performed over ten random-alloy configurations with fixed interatomic exchange parameters.

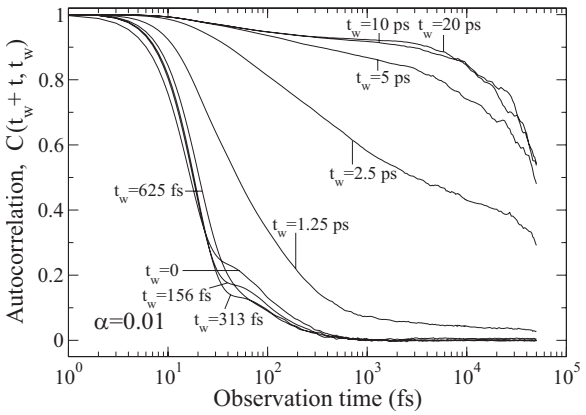

FIG. 1. Autocorrelation $C(t_w+t,t_w)$ calculated for CuMn after a quench from completely random spin orientations to $T=10$ K with damping $\alpha=0.01$. The autocorrelation is presented (from left to right in the figure) for the logarithmically spaced waiting times $t_w=0$, 1.56×10^2, 3.13×10^2, 6.25×10^2, 1.25×10^3, 2.5×10^3, 5×10^3, 1×10^4, and 2×10^4 fs.

The main concern of the current work is to investigate the influence of damping on the aging behavior and on spin relaxation in general. First, let us consider two limiting cases:

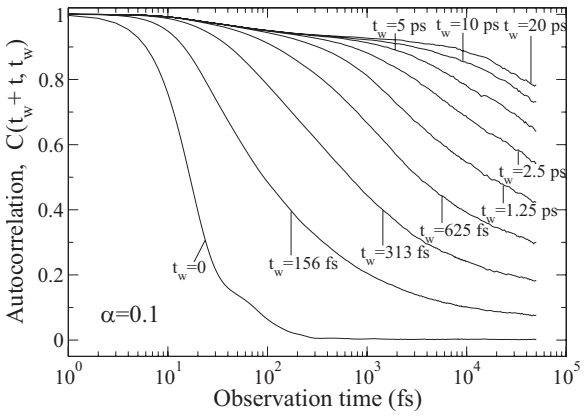

FIG. 2. Same as Fig. 1 but with damping $\alpha=0.0316$.

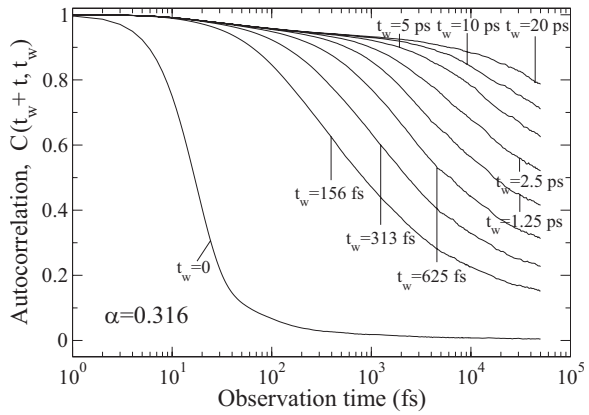

FIG. 3. Same as Fig. 1 but with damping $\alpha=0.1$.

$\alpha=0$ and $\alpha=\infty$. The first case is trivial and corresponds to an utterly deterministic evolution with the total energy conserved. We can call this a "microcanonical dynamics" for brevity. Since there is no coupling to a heat bath, the system will never reach equilibrium in this type of dynamics. In case of the infinite damping parameter, on the other hand, relaxation of a spin to equilibrium with respect to its local magnetic field occurs instantaneously, and spin dynamics becomes equivalent to the dynamics of the heat-bath Monte Carlo method.[38] For intermediate values of the damping parameter, we expect a system to cross over from the initial off-equilibrium dynamics to the regime of relaxation toward a (quasi)equilibrium state. The duration of the crossover must be dependent on the damping parameter.

In Figs. 1–4 we show the spin-glass dynamics of CuMn for four different damping parameters, $\alpha=0.01, 0.0316, 0.1, 0.316$, respectively. We plot the autocorrelation function for logarithmically spaced waiting times. Note that time is given in femtoseconds but the time step is 0.01 fs. In all four cases the autocorrelation for $t_w=0$ illustrates the initial dynamics of the system right after the quench. The behavior at short times ($t \lesssim 500$ fs) is similar for all values of α and is shown in Fig. 5 in logarithmic-linear scale. The evolution of the autocorrelation function can be described here as a sum of two exponents followed by a slower-than-exponential decay at larger times. That is for $t \lesssim 200$ fs, we have

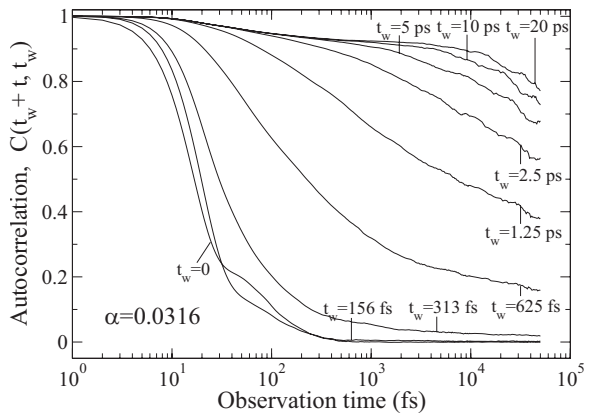

FIG. 4. Same as Fig. 1 but with damping $\alpha=0.316$.

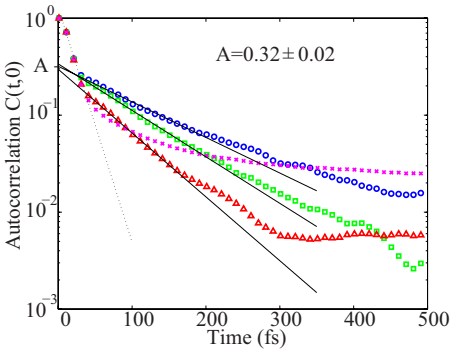

FIG. 5. (Color online) Autocorrelation $C(t, t_w=0)$ for four values of the damping parameter: $\alpha=0.01$ (circles), $\alpha=0.0316$ (boxes), $\alpha=0.1$ (triangles), and $\alpha=0.316$ (crosses). The dashed line is a linear fit to the points for 10 fs $\leq t \leq$ 40 fs; the slope is equal to $1/\tau_1$ of Eq. (12). The slope of the solid lines corresponds to the damping relaxation rate $1/\tau_2$ in Eq. (12).

$$C(t,0) \approx (1-A)e^{-t/\tau_1} + Ae^{-t/\tau_2}, \tag{12}$$

where the value of A can be extracted from the crossing point of the straight lines corresponding to the second exponent: $A=0.32\pm0.02$. The bump in Figs. 1–4 on the curves for $t_w=0$ corresponds to the second term in Eq. (12). The initial slope of the curves, $1/\tau_1$, is independent of damping (see Fig. 5) and temperature (data not shown) and depends only on the details of the Hamiltonian and initial spin distribution. When the initial distribution is random, as is the case in our simulations, the drop of the autocorrelation is dominated by a strong precessional motion of the atomic spins in rapidly varying effective exchange fields. As the directions of the effective fields are initially oriented in a completely random fashion, the angle between the atomic spin and its effective field is on average large, resulting in a large precessional torque on the atomic spins. The system gradually relaxes by means of a damping torque on each atomic spin, with the energy of the system dropping down from a high value of the random spin configuration ("high-temperature" phase) to a value close to the average energy for $T=10$ K.

A subsequent decay of the autocorrelation is associated with equilibration of spins in their local fields. Clearly, the rate of the relaxation, $1/\tau_2$, depends strongly on the value of the damping parameter and for this reason we refer to it as "the damping relaxation." As the rate $1/\tau_2$ diminishes with increasing α, the initial damping relaxation becomes more difficult to identify. As seen in Fig. 5 from the evolution of the autocorrelation for $\alpha=0.316$, the crossover from the initial stage to a nonexponential decay is rather smooth and the relaxation due to damping is indistinguishable.

The rate of the damping relaxation affects the behavior of the autocorrelation function for waiting times much larger than the value of τ_2. From Fig. 1 one can see that for $\alpha=0.01$ the curves fall on top of each other for waiting times up to $t_w=625$ fs. This implies that, up to this moment, the decay of the autocorrelation function is time-translation invariant. In fact, it seems that with this value of the damping parameter, the system never enters the aging regime and the initial relaxation phase crosses over directly to relaxation to

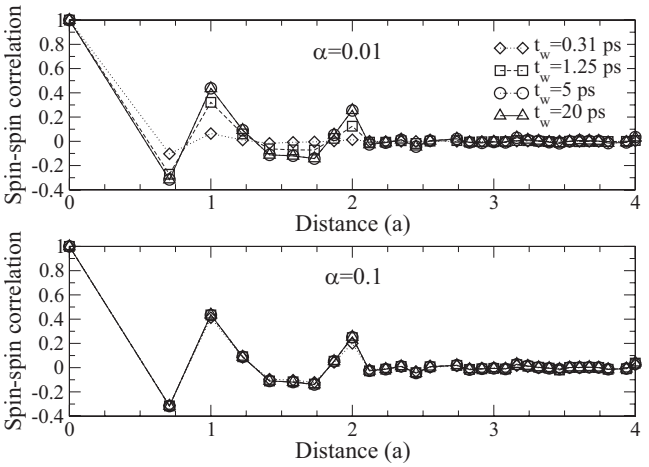

FIG. 6. The calculated spin-spin correlation function, $\langle \mathbf{m}_i \cdot \mathbf{m}_j \rangle$, for $\alpha=0.01$ (upper panel) and $\alpha=0.1$ (lower panel). The correlation function is plotted for four logarithmically spaced waiting times. For $\alpha=0.1$, all four curves fall essentially on top of each other.

the global equilibrium for $t_w > 5$ fs. On the other hand, at smaller values of τ_2, the aging behavior recovers (see Figs. 3 and 4) and the spin dynamics becomes similar to that in the case of infinite damping. This implies that the strength of damping is determined by the ratio of the time scale τ_2 of the damping relaxation and the characteristic time of detuning of local fields due to the motion of neighboring spins contributing to these local fields.

To determine to what extent the system has equilibrated, one can look at the evolution of the spin-spin correlation function $g(\mathbf{r}_{ij}) = \langle \mathbf{m}_i \cdot \mathbf{m}_j \rangle$. In Fig. 6 we plot $g(\mathbf{r}_{ij})$ as a function of the distance $|\mathbf{r}_{ij}|$ between the spins for different waiting times of the system. The correlation function is plotted both for $\alpha=0.01$ (upper panel) and $\alpha=0.1$ (lower panel). As expected from the autocorrelation, $g(\mathbf{r}_{ij})$ is seen to evolve faster the larger the damping parameter. It means that for sufficiently strong damping the system reaches the quasiequilibrium phase fast enough for the aging regime to establish.

The nonequilibrium behavior seen at small waiting times for small damping parameter values can be detected at the microscopic level by observing the trajectories of randomly selected spins. In Fig. 7 we plot trajectories of a typical atomic spin evolving during 100 fs (corresponding to a short-time scale) for $\alpha=0.01$ and $\alpha=0.1$, and for two different waiting times. The upper panel shows the trajectory for $\alpha=0.01$ after a waiting time of 1.25 ps. There is a large degree of precessional motion of the atomic spin, confirming the conclusions drawn from the behavior of the autocorrelation that the system is still in the initial relaxation phase at this waiting time. The middle panel shows the same system after a waiting time of 5 ps, showing an atomic spin with a much more stable spin direction. The spin is now either in equilibrium or on the verge of entering equilibrium although spin motion is much more pronounced here than in the aging regime for the system with $\alpha=0.1$. The lower panel shows the trajectory of an atomic spin for $\alpha=0.1$ at a waiting time of 1.25 ps. The system is in the aging regime here, as seen in Fig. 3, and the atomic spin direction is stable on a time scale of 100 fs.

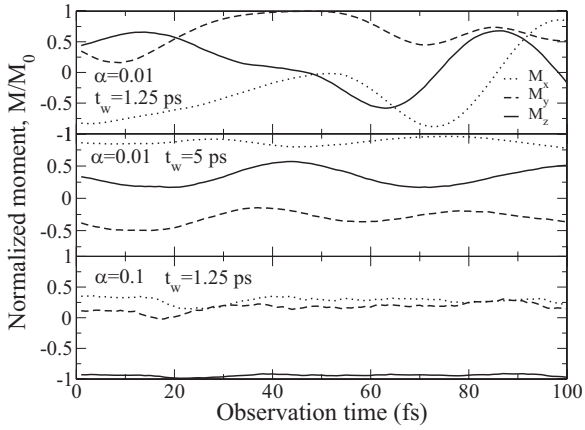

FIG. 7. The trajectory for one typical atomic spin at $t_w=1.25$ ps for $\alpha=0.01$ (upper panel), at $t_w=5$ ps for $\alpha=0.01$ (middle panel), and at $t_w=1.25$ ps for $\alpha=0.1$ (lower panel).

In the aging regime, the autocorrelation is characterized by an initial reduction in the autocorrelation on to a plateau, similar to what is seen for systems in equilibrium. A plateau is clearly seen in Figs. 1–4 for relatively large waiting times. The position of the plateau depends on temperature and is related to the spin-glass order parameter. More precisely,

$$\lim_{t\to\infty} \lim_{t_w\to\infty} C(t_w + t, t_w) = q_{\mathrm{EA}} \tag{13}$$

in the macroscopic limit, and the Edwards-Anderson order parameter, q_{EA}, is defined (again in the macroscopic limit) as

$$q_{\mathrm{EA}} = \frac{1}{N} \sum_i [\langle \mathbf{m}_i \rangle_T^2]_{\mathrm{av}}, \tag{14}$$

where $\langle \cdots \rangle_T$ stands for thermal averaging. Following the plateau, or the quasiequilibrium phase, is the aging phase. The crossover from one phase to another occurs at a time, t_s, when a sudden drop of the autocorrelation takes place. The time t_s can be best identified as the maximum of the relaxation rate defined by Eq. (7).

The relaxation rate for $\alpha=0.1$ and for a few waiting times is plotted in Fig. 8. The relaxation rate is obtained by calculating the derivative with respect to $\ln t$ of the autocorrelation. Note that the poorly defined peaks at the end of the observation time ($t \sim 10^4$ fs) are artifacts of a smearing scheme used when calculating the derivative and which breaks down close to the edge of the observation interval. In the inset we show the position of the peak relaxation rate, or t_s, with respect to the waiting time. As one can see, t_s is slightly larger than t_w, which is expected for the aging regime in a spin-glass system.[39] However, the total time window used in the simulations does not allow inferring of any definite form of the dependence.

B. Spin dynamics of the Heisenberg EA model for weak damping

To investigate even further spin dynamics for small values of α, we have performed simulations of the Heisenberg EA model for $\alpha=0.01$ and for different lattice sizes. The simu-

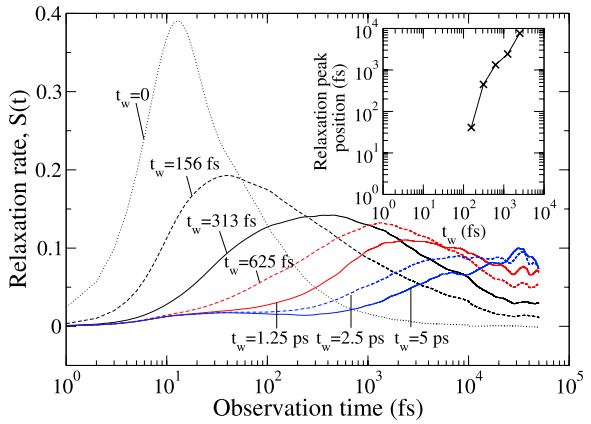

FIG. 8. (Color online) Relaxation rate, $S(t)$, for the simulation in Fig. 3 with $\alpha=0.1$. The relaxation rate is plotted for the logarithmically spaced waiting times $t_w=0$, 1.56×10^2, 3.13×10^2, 6.25×10^2, 1.25×10^3, 2.5×10^3, and 5×10^3 fs. The inset shows the relationship between the waiting time and the peak of the relaxation rate for the waiting times $t_w=1.56\times10^2$, 3.13×10^2, 6.25×10^2, 1.25×10^3, and 2.5×10^3 fs. For the last waiting time the largest peak seems to be a numerical artifact. Instead the second largest peak was chosen as input for the inset.

lations have been performed on a cubic lattice of different sizes $L\times L\times L$, where $L=4$, 8, and 16, and with random nearest-neighbor exchange interactions drawn from a Gaussian distribution with a standard deviation of 1 mRy. This is typically the order of exchange interactions in CuMn alloys. The freezing temperature, T_g, is expected to be 25 K for this model (0.16 within the dimensionless model).[40]

In Fig. 9 we show the calculated autocorrelation for a simulation of the Edwards-Anderson model. The simulated process is a relaxation following a quench from completely random spin orientations to 10 K (0.063 within the standard dimensionless model). The autocorrelation with respect to

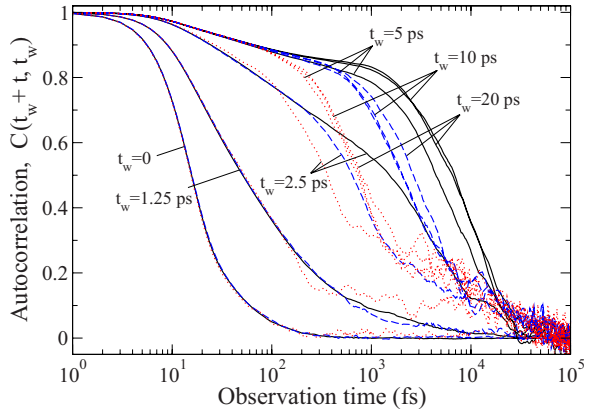

FIG. 9. (Color online) Autocorrelation $C(t_w+t,t_w)$ calculated for the Edwards-Anderson model after a quench from completely random spin orientations to $T=10$ K with $\alpha=0.01$. Different line styles and colors signify different system sizes: $4\times4\times4$ (dotted, red), $8\times8\times8$ (dashed, blue), and $16\times16\times16$ (full, black). For each system size the autocorrelation is presented (from left to right in the figure) for the logarithmically spaced waiting times $t_w=0$, 1.25×10^3, 2.5×10^3, 5×10^3, 1×10^4, and 2×10^4 fs.

observation time is plotted for several logarithmically spaced waiting times. As in the CuMn simulations, averaging was performed over ten different bond realizations, and for each bond configuration, ten simulations with different initial random spin distributions and different random number sequences in the Langevin equations have been done.

There are three sets of curves in Fig. 9 for three different system sizes. As seen in the figure, for the choice of the damping parameter ($\alpha=0.01$) and system sizes ($L=4,8,16$), the aging regime is very short or even nonpresent in these simulations. The global equilibrium is reached very soon after the initial relaxation was accomplished. It is also worth noting that there is a noticeable similarity between the waiting time dependence of the autocorrelation function for the $16\times16\times16$ EA model (Fig. 9) and the $32\times32\times32$ CuMn alloy simulated with the same damping parameter (Fig. 1). Moreover, comparing the curves corresponding to $t_w=0$, one can see that the initial phase is independent of the system size.

Typically, a spin-glass system enters the aging regime as soon as local equilibrium conditions are being met. The dynamics proceeds by a rearrangement of the magnetic order on a length scale corresponding to a time scale of the order of the age of the system. In this particular simulation, a pure aging regime cannot be identified as the system enters the global equilibrium soon after the initial relaxation. In contrast to equilibrium, within the aging regime the autocorrelation should depend on the waiting time and not on the system size. For the largest four waiting times in Fig. 9, we see the autocorrelation characterized by an initial reduction on to a plateau followed by a large sudden reduction to zero for different observation times depending on the size of the system.

V. CONCLUSIONS

The investigation of spin dynamics based on the realistic spin-glass model has been performed by solving the Langevin equations of motion. The exchange parameters have been calculated from first-principles DFT calculations while the damping parameter has been varied to study the influence of damping on the dynamics. In the first-principles theory no assumptions are made concerning the magnetic moments or interatomic exchange interactions; hence the calculated parameters of the model are materials specific. It is rewarding to observe that our model reproduces essential features of spin-glass systems. For instance, analogous studies on a different disordered system, namely, Mn-doped GaAs,[41] resulted in a different dynamical behavior although the geometry of the magnetic subsystem (fcc sublattice) is the same as in our model.

The simulations showed that, below the spin-freezing temperature, T_g, the system exhibits the aging behavior for sufficiently large values of the damping parameter, α. In this case, the dynamics is very similar to that obtained from corresponding Monte Carlo simulations. For weak damping, we find that the behavior is different and can be characterized by two regimes for small and large waiting times, respectively. For waiting times, t_w, below some certain value, the autocor-

relation function does not depend on t_w (i.e., it is time-translation invariant) and hence is the same as for $t_w=0$. For waiting times above a certain limit, the autocorrelation is also time-translation invariant but is characterized by a much slower decay. The time-translation invariance of the autocorrelation suggests that a system of finite size reaches equilibrium faster at weaker damping. As a result, it becomes clear that spin dynamics inside moderately sized domains in spin glasses can be strongly affected by damping.

A direct experimental observation of the effects of weak damping described here may be hampered by the large difference in time scales accessible in the presented numerical simulations and real-life experiments. However, this seems to be not completely impossible, taking into account that spin-echo experiments,[42] with its ability to probe time scales down to 10^{-12} s (compared to 10^{-13} in our simulations), can potentially shed light on the short-time behavior of spin-glass systems. Besides, it follows from our studies that dynamics on even larger time scales may be modified because of weak magnetic damping.

Moreover, the similarity between our nonequilibrium results to those found in Monte Carlo studies using simpler model Hamiltonians verifies the usefulness of those methods in mimicking real spin glasses on short-time scales. This hints that a corresponding agreement is valid on longer time scales, and thus our results indirectly support the relevance of simulations on "simple" model systems using special purpose computers[43] that close the previously huge time scale gap between the nonequilibrium dynamics probed in simulations and experiments on real spin glasses.

ACKNOWLEDGMENTS

Financial support from the Swedish Foundation for Strategic Research (SSF), Swedish Research Council (VR), Royal Swedish Academy of Sciences (KVA), Liljewalchs Resestipendium, and Wallenbergstiftelsen is acknowledged. Calculations have been performed at the Swedish national computer centers UPPMAX, HPC2N, and NSC.

*oleg.peil@fysik.uu.se

[1] K. Binder and A. Young, Rev. Mod. Phys. **58**, 801 (1986).
[2] *Spin Glasses and Random Fields*, edited by A. P. Young (World Scientific, Singapore, 1998).
[3] R. G. Palmer, Adv. Phys. **31**, 669 (1982).
[4] L. Lundgren, P. Svedlindh, P. Nordblad, and O. Beckman, Phys. Rev. Lett. **51**, 911 (1983).
[5] D. S. Fisher and D. A. Huse, Phys. Rev. B **38**, 373 (1988).
[6] A. T. Ogielski and D. L. Stein, Phys. Rev. Lett. **55**, 1634 (1985).
[7] S. Teitel and E. Domany, Phys. Rev. Lett. **55**, 2176 (1985).
[8] B. A. Huberman and M. Kerszberg, J. Phys. A **18**, L331 (1985).
[9] P. Sibani and K. H. Hoffmann, Phys. Rev. Lett. **63**, 2853 (1989).
[10] J.-P. Bouchaud and D. S. Dean, J. Phys. I **5**, 265 (1995).
[11] S. F. Edwards, and P. W. Anderson, J. Phys. F: Met. Phys. **5**, 965 (1975).
[12] J.-O. Andersson, J. Mattsson, and P. Svedlindh, Phys. Rev. B **46**, 8297 (1992).
[13] Y. Ozeki and N. Ito, Phys. Rev. B **64**, 024416 (2001).
[14] H. G. Katzgraber and I. A. Campbell, Phys. Rev. B **72**, 014462 (2005).
[15] R. E. Blundell, K. Humayun, and A. J. Bray, J. Phys. A **25**, L733 (1992).
[16] A. T. Ogielski, Phys. Rev. B **32**, 7384 (1985).
[17] M. Picco, F. Ricci-Tersenghi, and F. Ritort, Eur. Phys. J. B **21**, 211 (2001).
[18] H. Rieger, J. Phys. A **26**, L615 (1993).
[19] L. Berthier and J. P. Bouchaud, Phys. Rev. B **66**, 054404 (2002).
[20] H. Kawamura, Phys. Rev. Lett. **90**, 237201 (2003).
[21] P. H. Poole, S. C. Glotzer, A. Coniglio, and N. Jan, Phys. Rev. Lett. **78**, 3394 (1997).
[22] S. C. Glotzer, N. Jan, T. Lookman, A. B. MacIsaac, and P. H. Poole, Phys. Rev. E **57**, 7350 (1998).
[23] H. E. Castillo, C. Chamon, L. F. Cugliandolo, and M. P. Kennett, Phys. Rev. Lett. **88**, 237201 (2002).
[24] C. Chamon, M. P. Kennett, H. E. Castillo, and L. F. Cugliandolo, Phys. Rev. Lett. **89**, 217201 (2002).
[25] L. R. Walker and R. E. Walstedt, Phys. Rev. Lett. **38**, 514 (1977).
[26] R. E. Walstedt and L. R. Walker, Phys. Rev. Lett. **47**, 1624 (1981).
[27] F. Matsubara and M. Iguchi, Phys. Rev. Lett. **68**, 3781 (1992).
[28] P. Monod and Y. Berthier, J. Magn. Magn. Mater. **15-18**, 149 (1980).
[29] P. M. Levy and A. Fert, Phys. Rev. B **23**, 4667 (1981).
[30] J. Kisker, L. Santen, M. Schreckenberg, and H. R. Rieger, Phys. Rev. B **53**, 6418 (1996).
[31] K. Yosida, Phys. Rev. **106**, 893 (1957).
[32] V. Kamberský, Czech. J. Phys., Sect. A **26**, 1366 (1976).
[33] B. Skubic, J. Hellsvik, L. Nordström, and O. Eriksson, J. Phys.: Condens. Matter **20**, 315203 (2008); http://www.fysik.uu.se/cmt/asd/
[34] A. V. Ruban, S. Shallcross, S. I. Simak, and H. L. Skriver, Phys. Rev. B **70**, 125115 (2004).
[35] L. Vitos, Phys. Rev. B **64**, 014107 (2001).
[36] P. Gibbs, T. M. Harden, and J. H. Smith, J. Phys. F: Met. Phys. **15**, 213 (1985).
[37] O. E. Peil, A. V. Ruban, and B. Johansson, New J. Phys. **10**, 083026 (2008).
[38] J. A. Olive, A. P. Young, and D. Sherrington, Phys. Rev. B **34**, 6341 (1986).
[39] V. S. Zotev, G. F. Rodriguez, G. G. Kenning, R. Orbach, E. Vincent, and J. Hammann, Phys. Rev. B **67**, 184422 (2003).
[40] L. Berthier and A. P. Young, Phys. Rev. B **69**, 184423 (2004).
[41] J. Hellsvik, B. Skubic, L. Nordström, B. Sanyal, O. Eriksson, P. Nordblad, and P. Svedlindh, Phys. Rev. B **78**, 144419 (2008).
[42] F. Mezei and A. P. Murani, J. Magn. Magn. Mater. **14**, 211 (1979).
[43] F. Belletti *et al.*, Phys. Rev. Lett. **101**, 157201 (2008).